Chaotic Nonlinear Stimulated Brillouin Scattering

C. J. Randall[a] and J. R. Albritton
Lawrence Livermore National Laboratory, Livermore, California 94550
(Received 12 September 1983)

Stimulated Brillouin scattering is analyzed in finite systems which have a boundary reflective to light. The linear instability is considerably altered from that for the usual transmitting boundaries. In the nonlinear regime the scattered light intensity may behave chaotically in time and exhibit rich frequency spectra including shifts corresponding to fractional harmonics of the fundamental acoustic wave. Simulation results compare favorably with data from laser-plasma–interaction experiments.

PACS numbers: 52.35.Mw, 42.65.Cq, 52.35.Py, 52.35.Ra

An intense laser light wave propagating in a material medium is unstable to decay into a scattered light wave and one of several waves supported by the material. Stimulated Brillouin scatter (SBS),[1] in which the material wave is acoustic, has been observed in a variety of media,[2] including plasmas.[3] In the usual analysis of SBS,[1,4] outgoing-wave conditions are applied to the decay waves at the material boundaries or at infinity. In fact, physical systems often possess a reflective boundary such as the critical surface in a laser-produced plasma.

Here we show that a boundary which is reflective to light waves induces significant new SBS phenomena. In the linear regime, we find large changes in the absolute instability threshold, growth rate, scattered-light frequency shift, and spatial envelopes of the unstable waves. In the nonlinear regime the scattered light intensity may behave chaotically in time and exhibit a rich frequency spectrum including shifts corresponding to both multiple and *fractional* harmonics of the fundamental acoustic wave frequency. This is in sharp contrast to the usual nonlinear steady-state picture of coupled fundamental waves.[3–6]

Chaotic behavior has been observed in many nonlinear dynamical systems,[7] and universal patterns have emerged.[8] Here, as the pump intensity, acoustic dissipation, and system length are varied, the time asymptotic behavior of the system, as evidenced by the intensity of the scattered light, for example, displays transitions among simple oscillatory steady states, complex limit cycles, and chaos of no discernible periodicity.

For parameters typical of high-intensity laser-plasma–interaction experiments, SBS is often in the chaotic regime. Highly structured scattered light spectra which are simulated in this regime compare favorably with experimental data.[9]

These new results establish that nonlinear SBS may be intrinsically nonsteady, so that modeling laboratory events requires at least the description that we shall present.

Our results may be understood by considering that a reflective boundary alters not only the equilibrium in which SBS grows but also the wave-coupling process of the instability itself. The reflected incident wave acts as a second counterpropagating pump so that an acoustic wave satisfies the frequency and wave-number matching conditions for three-wave coupling with the pumps and both Stokes (destabilizing) and anti-Stokes (stabilizing) backscattered light waves. Additionally, the beating of the two pumps supports a perturbation of the medium which in turn couples them together.[10] Thus the reflective boundary couples scattered light waves of the same frequency directly, and couples them indirectly as they propagate through the perturbation supported by the incident and reflected pumps. For these reasons, the system including the reflective boundary may be expected to display new stable and unstable behavior.

To demonstrate these effects, we analyze SBS in a homogeneous medium at rest with respect to the reflective boundary. We write the left and right propagating electromagnetic vector potentials and the (linear) acoustic response as products of a slowly varying envelope and a rapidly varying phase:

$$A(x,t) = \mathrm{Re}[A_+ \exp i(kx - \omega_0 t) + A_- \exp i(-kx - \omega_0 t)],$$

$$m(x,t) = \mathrm{Re}[\tilde{m} \exp(-2ikx)].$$

Here $\omega_0(k)$ is the laser pump frequency (wave number). In the dimensionless units of previous workers,[4] the envelopes obey the equations

$$\epsilon \frac{\partial A_\pm}{\partial t} + \frac{\partial A_\pm}{\partial x} = -iA_\mp \tilde{m}^{(*)}, \tag{1}$$

$$\frac{\partial^2 \tilde{m}}{\partial t^2} + 2\beta \frac{\partial \tilde{m}}{\partial t} + 2i\Omega_s \frac{\partial \tilde{m}}{\partial x} + \Omega_s^2 \tilde{m} = -2\Omega_s A_- A_+^*. \tag{2}$$

Here x is measured in units of the growth length $L_1=(c_s c_t)^{1/2}/\gamma_0$, t in units of $t_1=1/\gamma_0\sqrt{\epsilon}$, $\Omega_s=\omega_s t_1$, $\beta=\nu t_1/2$, and the superscript $(*)$ means conjugate for the $(+)$ equation only. In these units c_s (c_t) is the ion sound speed (group velocity of light), ω_s (ν) is the real frequency (damping rate) of undriven acoustic waves, γ_0 is the infinite-medium SBS growth rate, and $\epsilon=c_s/c_t$ is a small parameter.

In analyzing the linear regime of instability we split $A_\pm$ into the incident and reflected pump waves, $A_{\pm 0}$, and the Stokes, $C_\pm$, and anti-Stokes, $D_\pm$, backscattered waves. Similarly, we split the acoustic response $\tilde{m}$ into the perturbation supported by the beat of the pumps, $\tilde{m}_0$, and left- and right-going waves, $\tilde{m}_\pm$:

$$A_\pm(x,t)=A_{\pm 0}(x)+C_\pm(x,t)\exp(i\Omega t)+D_\pm(x,t)\exp(-i\Omega^* t),$$

$$\tilde{m}(x,t)=\tilde{m}_0(x)+\tilde{m}_+(x,t)\exp(i\Omega t)+\tilde{m}_-(x,t)\exp(-i\Omega^* t).$$

Substitution into Eqs. (1) and (2) results in a system of nine equations for the three equilibrium quantities, $A_{\pm 0}$ and $\tilde{m}_0$, and the six decay waves, $C_\pm$, $D_\pm$, and $\tilde{m}_\pm$. Let the boundary, of reflectivity f, be located at $x=0$ and the laser incident from the right at $x=L$; we take $A_{-0}(L)=1$ and $A_{+0}(0)=fA_{-0}(0)$, $C_+(0)=fC_-(0)$, $D_+(0)=fD_-(0)$, $\tilde{m}_+(0)=0$, and $\tilde{m}_-(L)=C_-(L)=D_-(L)=0$.

To investigate instability, we have set $\Omega=\Omega_s$, neglected $\partial^2/\partial t^2$ ($\Omega_s>\partial/\partial\tau=\Delta\Omega-i\gamma$), and computed the temporal evolution of the envelopes numerically. Figure 1(a) is contour plot of the growth rate, $\gamma(\epsilon,\Omega_s)$, for $L=10$, $|f|^2=0.9$, $\beta=0$. In the absence of a reflective boundary ($f=0$), $\gamma=2$ nearly independent of ϵ and Ω_s. It is evident that the reflective boundary has induced substantial variation of the growth rate with ϵ and Ω_s. For example, at point A (coordinates $\Omega_s=55$, $\epsilon=0.001$) the value of the growth rate is about 7.0, several times the usual value!

Figure 1(b) displays $\Delta\Omega(\epsilon,\Omega_s)$, the departure of the frequency of the Stokes wave from its usual value of the pump frequency shifted by the acoustic frequency. The reflective boundary induces large departures as may be seen for example at point A, where $\Delta\Omega=-10$. In physical units this corresponds to a total Stokes frequency shift of $-1.2\omega_s$.

In Figs. 2(a) and 2(b) we display the amplitudes of the electromagnetic, $|C_\pm|^2$ and $|D_\pm|^2$, and acoustic, $|\tilde{m}_\pm|^2$, eigenfunctions obtained for point A in Fig. 1. Figures 2(c) and 2(d) show $|C_-|^2$ and $|m_-|^2$ for the same parameters except that $f=0$. With the reflective boundary the acoustic waves fill the system whereas in the $f=0$ case they are appreciable only over a few growth lengths. The anti-Stokes light wave, $|D_+|^2$, exits from the region with almost one-tenth the intensity of the Stokes wave, $|C_+|^2$.

In pursuing the foregoing analysis into the nonlinear regime we take up more general equations[6] which are appropriate for drifting, inhomogeneous media and allow comparison with data from laser-

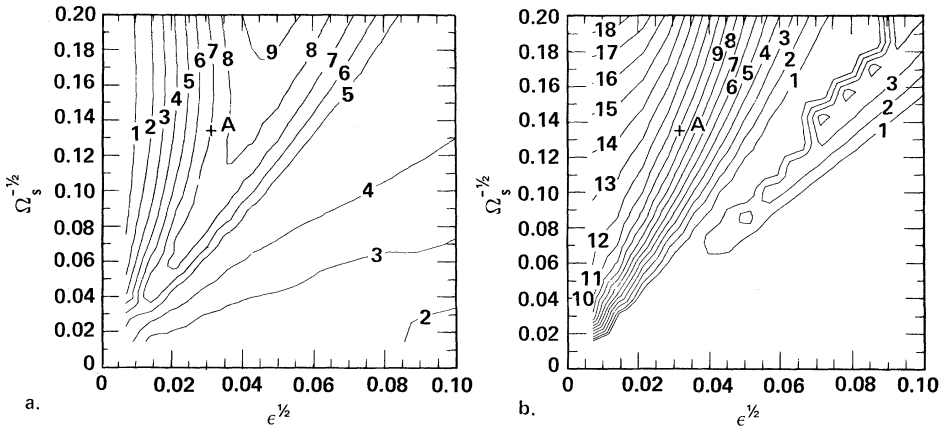

FIG. 1. (a) Contour plot of the normalized SBS growth rate, $\gamma(\epsilon,\Omega_s)$, in the presence of a reflective internal boundary: $L=10$, $|f|^2=0.9$, $\beta=0$. The point labeled A (cited in the text) has coordinates $\Omega_s=55$, $\epsilon=0.001$. (b) Contour plot of the normalized SBS frequency shift, $\Delta\Omega(\epsilon,\Omega_s)$, relative to the usual value.

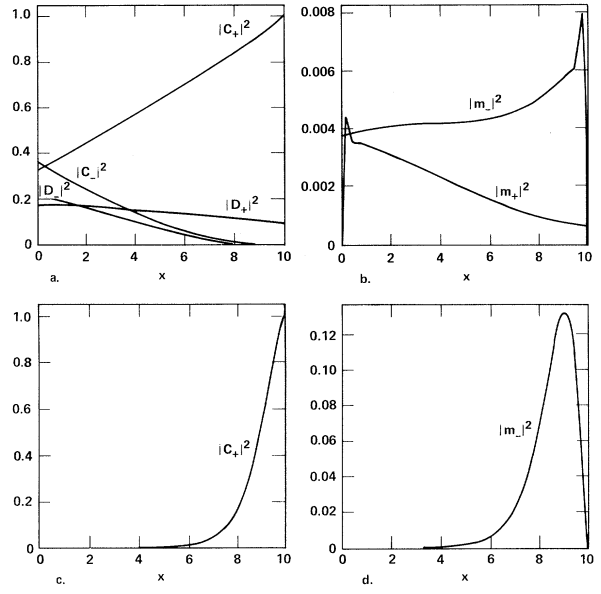

FIG. 2. (a) Amplitudes of the electromagnetic eigenfunctions, $|C_{\pm}|^2$, and $|D_{\pm}|^2$, of point A in Fig. 1. (b) Amplitudes of the corresponding acoustic eigenfunctions, $|m_{\pm}|^2$. (c) $|C_-|^2$ and (d) $|m_-|^2$ for the same parameters except that $f=0$. In both cases the normalization is that $C_+(L)=1$.

plasma–interaction experiments:

$$\frac{\partial A_{\pm}}{\partial t} \pm c_t \frac{\partial A_{\pm}}{\partial x} = -i\gamma_0 A_{\mp} \tilde{m}^{(*)}, \tag{3}$$

$$\frac{d^2\tilde{m}}{dt^2} - 2i\omega_s\left[\left(\eta + i\frac{\nu}{2\omega_s}\frac{d\tilde{m}}{dt}\right) - c_s\frac{\partial\tilde{m}}{\partial x}\right] - \omega_s^2\left(\eta^2 - 1 + i\frac{\nu}{\omega_s}\right)\tilde{m} = -2\omega_s\gamma_0 A_- A_+^*. \tag{4}$$

In Eq. (4), $d/dt = \partial/\partial t + v_0\partial/\partial x$ is the convective derivative in the drifting medium (drift velocity v_0 in the laboratory frame where the scattered light spectra are observed), and $\eta = \Delta\omega/\omega_s + v_0/c_s$, where $\Delta\omega = \omega_- - \omega_+$ is the frequency difference of the left- and right-going light waves induced by plasma expansion.[11] Frequency shifts due to SBS are contained in the phases of the envelopes $A_{\pm}$.

In Fig. 3 we display numerical solutions of Eqs. (3) and (4) for a homogeneous stationary plasma slab. In the units of our preceding analysis, the parameters are $L=10$, $|f|^2=0.9$, $\Omega_s=28$, $\epsilon=0.001$, and $\beta=3.0$. Figure 3(a) is a time history of the scattered/reflected light, $A_s=(A_+-A_{+0})/A_{+0}$, emerging at $x=L$. Using Fig. 1 we estimate a linear growth rate of $\gamma\cong\gamma(\epsilon,\Omega_s)-\beta=7.3-3.0=4.3$, the difference between the growth rate

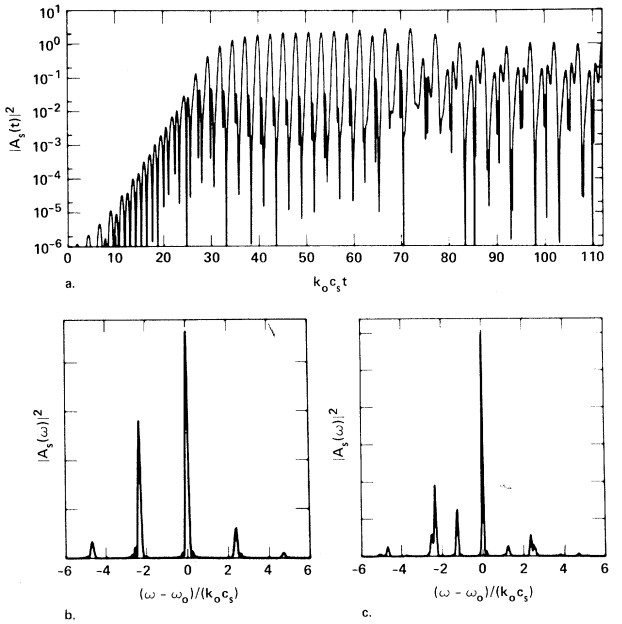

FIG. 3. (a) Time history of the scattered light, $A_s(t)=[A_+(t)-A_{+0}]/A_{+0}$, emerging at $x=L$, showing linear growth, saturation, and asymptotic limit-cycle behavior. (b) Frequency spectrum, $A_s(\omega)$, prior to saturation. The Stokes and anti-Stokes lines at $\Delta\omega=\pm 2.5k_0c_s$ are prominent, and the nonlinearly generated multiple harmonics have emerged. (c) Frequency spectrum in the asymptotic state. Half-harmonics are clearly visible at $\Delta\omega=\pm 1.25k_0c_s$.

in the absence of damping and the damping rate, and a total frequency shift of $\Omega\cong-\Omega_s-\Delta\Omega(\epsilon,\Omega_s)=-28-14=-42$. Converting to the units of Fig. 3, we obtain $\gamma=0.26k_0c_s$ and $\omega-\omega_0=-2.5k_0c_s$ which agree well with the observed linear growth rate and frequency shift. After saturation at $t=30(k_0c_s)^{-1}$, the instability evolves slowly toward its asymptotic state, a complex limit cycle, characterized by multiple and *half*-harmonics (period doubling) of the linear frequency shift! This state was not anticipated by the usual nonlinear steady-state theory.[3-6]

As the system parameters are varied (particularly as L is increased), the asymptotic limit-cycle behavior can become more and more complex, with smaller fractional harmonics and their multiples being generated. Finally, the asymptotic state can become chaotic, i.e., not discernibly periodic, and exhibit highly structured frequency spectra. Such chaotic behavior is shown in Figs. 4(a) and 4(b).

The systems which exhibit chaotic SBS are not limited to simple homogeneous ones. In fact, the background plasma conditions in the calculation which produced Figs. 4(a) and 4(b) are those of re-

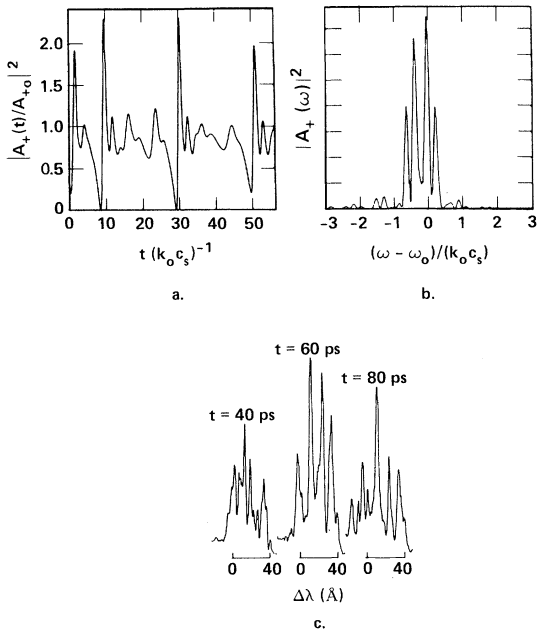

FIG. 4. (a) Time history of the scattered/reflected intensity, $|A_+(t)|^2$, showing chaotic behavior; from the simulation of a high-intensity laser-plasma–interaction experiment. (b) Calculated frequency spectrum of the scattered/reflected light, $|A_+(\omega)|^2$, near the peak of the laser pulse. (c) Experimental scattered/reflected light spectra from Turner and Goldman (Ref. 9). The spectrum labeled 60 ps corresponds to the peak of the laser pulse.

cent high-intensity short-pulse, laser-plasma–interaction experiments.[9] The qualitative similarity between the light spectra from the simulation, Fig. 4(b), and the experimental data, Fig. 4(c), is striking. Moreover, the agreement can be made semiquantitative. At peak laser intensity, 5×10^{15} W/cm^2 at 60 ps, the simulation employs an electron temperature of 15 keV. The normalized sound speed at this temperature is $\epsilon = c_s/c = 2.8\times10^{-3}$. The calculated frequency shifts in Fig. 4(b) are converted to wavelength shifts of Nd-laser light by multiplying by $-\lambda_0\epsilon = -30$ Å. Thus both the relative spacing and the placement of the peaks in the simulation spectrum are in agreement with experiment. If one appeals to multiple (rather than fractional) harmonic generation to explain the experimental spectra, the sound speed derived from the spacing of the spectrum peaks, $c_s/c = \Delta\lambda/2\lambda$, yields an electron temperature of ~ 0.4 keV which is much too low for the experimental conditions.

This work was performed under the auspices of the U. S. Department of Energy by the Lawrence Livermore National Laboratory under Contract No. W-7405-ENG-48.

[a]Present address: Schlumberger-Doll Research, P. O. Box 307, Ridgefield, Conn. 06877.

[1]N. W. Kroll, J. Appl. Phys. **36**, 34 (1965).

[2]R. Y. Chiao, B. P. Stoicheff, and C. H. Townes, Phys. Rev. Lett. **12**, 592 (1964); E. E. Hagenlocker, R. W. Minck, and W. G. Rado, Phys. Rev. **154**, 226 (1967).

[3]D. W. Phillion, W. L. Kruer, and V. C. Rupert, Phys. Rev. Lett. **39**, 1529 (1977); B. H. Ripin, F. C. Young, J. A. Stamper, C. M. Armstrong, R. Decoste, E. A. McLean, and S. E. Bodner, Phys. Rev. Lett. **39**, 611 (1977); R. E. Turner and L. M. Goldman, Phys. Rev. Lett. **44**, 400 (1980).

[4]D. W. Forslund, J. M. Kindel, and E. L. Lindman, Phys. Fluids **18**, 1002 (1975).

[5]T. Speziale, J. F. McGrath, and R. L. Berger, Phys. Fluids **26**, 1275 (1980).

[6]C. J. Randall, J. J. Thomson, and K. G. Estabrook, Phys. Rev. Lett. **43**, 924 (1979); C. J. Randall, J. R. Albritton, and J. J. Thomson, Phys. Fluids **24**, 1474 (1981).

[7]H. M. Gibbs, F. A. Hopf, D. L. Kaplan, and R. L. Shoemaker, Phys. Rev. Lett. **46**, 474 (1981); B. A. Huberman, J. P. Crutchfield, and N. H. Packard, Appl. Phys. Lett. **37**, 750 (1980).

[8]M. J. Feigenbaum, J. Stat. Phys. **21**, 669 (1979).

[9]R. E. Turner and L. M. Goldman, Phys. Fluids **24**, 184 (1981); F. Martin, J. Sabbagh, H. Pepin, and P. Lavigne, in Proceedings of the Fifteenth European Conference on Laser Interaction with Matter, Garching, Federal Republic of Germany, 1982 (unpublished), FC4.

[10]If the medium and reflective boundary have a relative velocity which is near sonic, large energy transfers from the incident to the reflected pump wave can occur so that transmission to the internal boundary is reduced considerably (Ref. 6).

[11]T. Dewandre, J. R. Albritton, and E. A. Williams, Phys. Fluids **24**, 528 (1981).